

Developing soft-computing regression model for predicting bearing capacity of eccentrically loaded footings on anisotropic clay



Kongtawan Sangjinda^a, Rungkhun Banyong^a, Saif Alzabeebee^b, Suraparb Keawsawasvong^{a,*}

^a Research Unit in Sciences and Innovative Technologies for Civil Engineering Infrastructures, Department of Civil Engineering, Faculty of Engineering, Thammasat School of Engineering, Thammasat University, Pathumthani, 12120, Thailand

^b Department of Roads and Transport Engineering, University of Al-Qadisiyah, Al-Diwaniyah, Al-Qadisiyah, Iraq

ARTICLE INFO

Keywords:

Bearing capacity
Anisotropic clay
Footing
FELA
MOGA-EPR

ABSTRACT

In this investigation, the bearing capacity solution of a strip footing in anisotropic clay under inclined and eccentric load is analyzed using the numerical simulation model. The lower and upper bound finite element limit analysis (FELA) approaches are utilized to establish precise modeling and derive the numerical outcomes of a strip footing's bearing capacity. All analyses use effective automated adaptive meshes with three iteration stages to enhance the accuracy of the outcomes. The parametric analysis is performed to examine the influence of four dimensionless parameters which are taken into account in this study, namely the anisotropic strength ratio, the dimensionless eccentricity, the load inclination angle, and the adhesion factor to the bearing capacity factor. Furthermore, a new model has been proposed to predict the bearing capacity factor for the calculation of the undrained bearing capacity for footings resting on an anisotropic clay using an advanced data-driven method (MOGA-EPR). The new model takes into account the anisotropy, eccentricity, and inclination of the applied load and could be used with confidence in routine designs of shallow foundations in undrained conditions with the consideration of the anisotropic strengths of clays.

1. Introduction

The foundation is a primary structure that requires attention due to the mechanisms which transfer load from the upper structure to the ground. The foundation must function in accordance with safety and reliability requirements so that the building or machinery it supports can achieve its intended function under typical working loads. The fundamental concept of the bearing capacity solution was initially introduced by Terzaghi (1943). He proposed the bearing capacity factors considering the effects of soil cohesion, soil unit weight, and surcharge which are taken into account by based on the Mohr-Coulomb failure criterion model. Nevertheless, visualizing a foundation with only a vertical load operating on it at its center is a hypothetical illustration and an enormous simplification. In general, a multi-story structure can transfer horizontal loads to the substructure apart from the vertical load caused by its own weight, such as wind loads or concrete cantilevered components. Furthermore, the load's application may not be exact in the foundation's center. Thus, it is crucial to consider the effects of inclination and eccentricity of the weight applied. The supports of marine

vessels ports, radio towers, overpasses, and offshore structures are just several examples of unusual structures that are frequently exerted by eccentric longitudinal lateral pressures.

Based on earlier studies, a number of researchers including Meyerhof (1955; 1963), Hansen (1970), and Vesic (1975) have adopted Terzaghi's bearing capacity equation, that takes eccentricity and inclination loading into account by utilizing the framework of limit equilibrium and slip-line techniques. Consequently, the bearing capacity solutions of footings under eccentric loading are initially performed through a numerical framework namely Finite Element Analysis (FEA) for both cohesionless and cohesive soils (Taiebat and Carter, 2002; Loukidis et al., 2008). The discontinuity arrangement optimal control method was used by Zheng et al. (2019) to address the bearing capacity problems of the multi-layered strip foundation soils forced by inclined loads. A different numerical analysis known as Finite Element Limit Analysis (FELA) was carried out by Hjiaj et al. (2004) to explore the bearing capacity of foundations on cohesive-frictional soils with the consideration of the impacts of both inclination and eccentricity factors. The identical technique is being used by Krabbenhoft et al. (2012, 2014) to

* Corresponding author.

E-mail addresses: kongtawan.sang@dome.tu.ac.th (K. Sangjinda), rungkhun.ban@gmail.com (R. Banyong), Saif.Alzabeebee@gmail.com (S. Alzabeebee), ksurapar@engr.tu.ac.th (S. Keawsawasvong).

conduct the lower bound solutions of eccentrically loaded foundations on cohesionless soils.

Natural clays frequently exhibit particular rates of strength anisotropy though since the intrinsic and stress-induced anisotropy of clay. It is discovered that the primary principal stress in anisotropic clay should be directed forward into the vertical plane or depositional orientation according to the studies of Ladd (1991) and Ladd and Degroot (2003). Likewise, they described the correlations between three undrained shear strengths, which consist of triaxial compression (s_{uc}), triaxial extension (s_{ue}), and straight simple shear (s_{us}) to the clay plastic index (PI). In the initial formulations, Casagrande and Carillo (1944) and Lo (1965) identified an anisotropic undrained shear strength, which is influenced by the main principal stress's angulations with respect to the vertical plane. According to the summary of their investigation, Casagrande and Carillo (1944) and Lo (1965) established the elementary notion of anisotropic undrained shear strength. Furthermore, the Anisotropic Undrained Shear (AUS) model, which develops based on the generalized Tresca criterion was subsequently generated by Krabbenhoft et al. (2019). It is the ideal failure prototype for anisotropic undrained clay which has been successfully utilized to describe the natural clay behavior incorporate with FELA methods to clarify complicated geotechnical problems such as the stability of slopes (Shiau et al., 2022), cavities (Lai et al., 2022a), bearing capacity of foundations (Lai et al., 2022b, 2022c; Keawsawasvong, 2022; Van et al., 2022; Nguyen et al., 2023; Keawsawasvong et al., 2022), excavation stability (Yodsomjai et al., 2021a; Lai et al., 2021d; 2022d, 2023a), underground walls (Lai et al., 2022e, 2023), and pullout capacity of caissons and anchors (Jearnsiripongkul et al., 2022; Nguyen et al., 2022; Keawsawasvong et al., 2021a).

However, the study of the bearing capacity factor under eccentric loading that takes the anisotropy of the clay into consideration still remains to be discussed. The major purpose of this study is to consider the effect of undrained strength anisotropy on the footing bearing capacity under eccentric and inclination loading. The numerical analyzes are performed in this study employing the upper and lower bound FELA framework. Additionally, four input dimensionless parameters that have never been studied before are desired for the parametric studies. As a result, the issue regarding the strip footing's bearing capacity under eccentric and inclined loads is solved, and the effects of the parameters taken into consideration are discussed. The bearing capacity factors are presented in charts that can be comfortably applied in practice and may use as a valuable tool for further investigation.

2. Problem statement

The problem description of a strip footing placed on anisotropic clay where the eccentric and inclined load is applied to the footing is shown in Fig. 1. The strip footing has a width of B . There is an ultimate load (P) applied on the footing with the inclination angle of β as well as an eccentric length of e . The clay profile characteristics are prompted by the AUS failure criterion with a constant of unit weight (γ) on the premise of homogeneity and anisotropy. As described previously, in the AUS

model, there are three types of undrained shear strength including undrained shear strengths obtained from triaxial compression (s_{uc}), triaxial extension shear (s_{ue}), and direct simple shear (s_{us}) are taken into account which can be simplified into two ratios for simpler comprehension as Equations (1) and (2). To highlight the variation in undrained strength of clays in different directions, two anisotropic strength ratios, namely r_e and r_s , are introduced. These ratios quantify the relationship between three anisotropic shear strengths and emphasize the degree of undrained strength anisotropy in anisotropic clays as follows:

$$r_e = \frac{s_{ue}}{s_{uc}} \quad (1)$$

$$r_s = \frac{s_{us}}{s_{uc}} \quad (2)$$

These two ratios shown in Equations (1) and (2) can be interrelated by using the relation as shown below (Keawsawasvong and Ukritchon, 2022):

$$r_s = \frac{2r_e}{1 + r_e} \quad (3)$$

Besides, the adhesion factor (α) at the rigid plate interface ranges from 0.25 to 1 representing only the partially and fully rough contact surfaces of the footings. The smooth scenario is not taken into account because it is impossible to calculate the ultimate lateral force of a footing with $\alpha = 0$ because a smooth footing cannot withstand the horizontal force generated by the inclination angle. Note that the adhesion factor is a reduction factor at the interface of soil and footing. To model the footing, the rigid plate elements are employed in the simulation, where the footing is assumed to very rigid and the failure of the footing is not feasible. Thus, the rigid footing enables to fully transfer loads to the ground.

The parametric investigation is performed in this study by employing the variation of four dimensionless parameters which can be normalized to produce the bearing capacity factor ($P/s_{uc}B$) for strip footing in anisotropic clay with eccentric and inclined loads as follows:

$$\frac{P}{s_{uc}B} \propto f\left(r_e, \frac{e}{B}, \beta, \alpha\right) \quad (4)$$

where r_e represents the anisotropic strength ratio; e/B represents dimensionless eccentricity; β represents the load inclination angle; and α represents the adhesion factor. Due to the undrained condition, the density and the angle of soil internal friction are not considered in this study since we only focused on the undrained bearing capacity factor N_c . The numerical outcomes of the bearing capacity factor are established based on these selected practical ranges including $r_e = 0.5–1.0$; $e/B = 0–0.4$; $\beta = 45–90^\circ$; $\alpha = 0.25–1.00$, respectively. These ranges were chosen to cover the practical variations commonly encountered in design practice. Furthermore, the range of r_e has been considered in previous studies, reinforcing their relevance and applicability with different kinds of geotechnical problems (i.e. Shiau et al., 2022; Lai et al., 2022a; Lai et al., 2022b, 2022c; Keawsawasvong, 2022; Van et al., 2022; Nguyen et al., 2023; Keawsawasvong et al., 2022; Yodsomjai et al., 2021a; Lai et al., 2021d; 2022d, 2023a; Lai et al., 2022e, 2023).

For more specific data are summarized in Table 1.

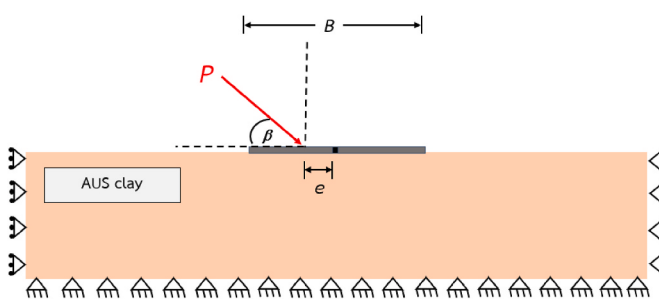


Fig. 1. Problem description of a strip footing on AUS clay.

Table 1
Input parameters.

Input parameters	Values	Average
e/B	0/0.1/0.2/0.3/0.4	0.2
α	0.25/0.5/0.75/1	0.625
$\beta (^\circ)$	45/60/75/90	67.5
r_e	0.5/0.6/0.7/0.8/0.9/1	0.75

3. Method of analysis

In order to conduct the precise numerical simulation, the FELA software OptumG2 is employed to simulate the numerical model of strip footing under eccentric and inclined loading. The typical model geometries for strip footing on anisotropic undrained clay under eccentric and inclined load is demonstrated in Fig. 2. Three distinct load inclination angles are chosen to compare the three models with $\beta = 45^\circ$, 60° , and 90° as shown in Fig. 2(a–c), respectively.

Note that the outcomes derived from the FELA technique exhibit a remarkable level of precision and accuracy. This is evident as the technique provides both upper bound and lower bound solutions, allowing for a narrow range of approximation that closely approaches the exact value. According to the study proposed by Sloan (2013), the Finite Element Limit Analysis (FELA), based on the limit analysis theory, relies solely on conventional strength parameters such as undrained shear strength while disregarding deformation parameters like Poisson's ratio and Young's modulus. FELA is primarily used for stability analysis, particularly for determining the collapse load or failure mechanisms of structures. It focuses on evaluating the maximum load-bearing capacity. This distinguishes FELA from conventional displacement-based Finite Element Methods (FEM). Unlike FEM, the FELA does not consider Poisson's ratio and Young's modulus in the analysis. The FELA technique does not provide the results of displacements, which is different

from the FEM method.

There are some specifications regarding the UB and LB simulation process that must be explained in accordance with the FELA software OptumG2 implementation. A six-noded triangle element is used to perform upper bound (UB) analysis, with each node containing two unknown velocities. The ultimate load on the foundations can be optimized using compatibility equations and velocity boundary conditions, which are included in the upper bound analysis. Additionally, the lower bound (LB) analysis uses a three-noded triangular element with three unknown stresses. The lower bound evaluation uses equilibrium equations with stress boundary conditions and no yield criteria violations. For the model boundary condition, the left and right boundaries are defined as roller supports, indicating that they allow movement in the vertical direction while preventing horizontal translation or rotation. The model's base boundary is defined as fixed support, implying complete restraint against both translation and rotation. The top ground surface, however, is designed to be unrestricted and unhindered, suggesting that it is free to move and deform without any imposed restraints.

Likewise, the rigid plate element is used to represent the footing and rigid-perfectly plastic AUS material is used to represent the clay layer encircling the footing in the local domains. The global domain capacity must also be adequate to avoid the interaction of failure zone between those boundaries. The fan mesh feature is implemented at the borders of

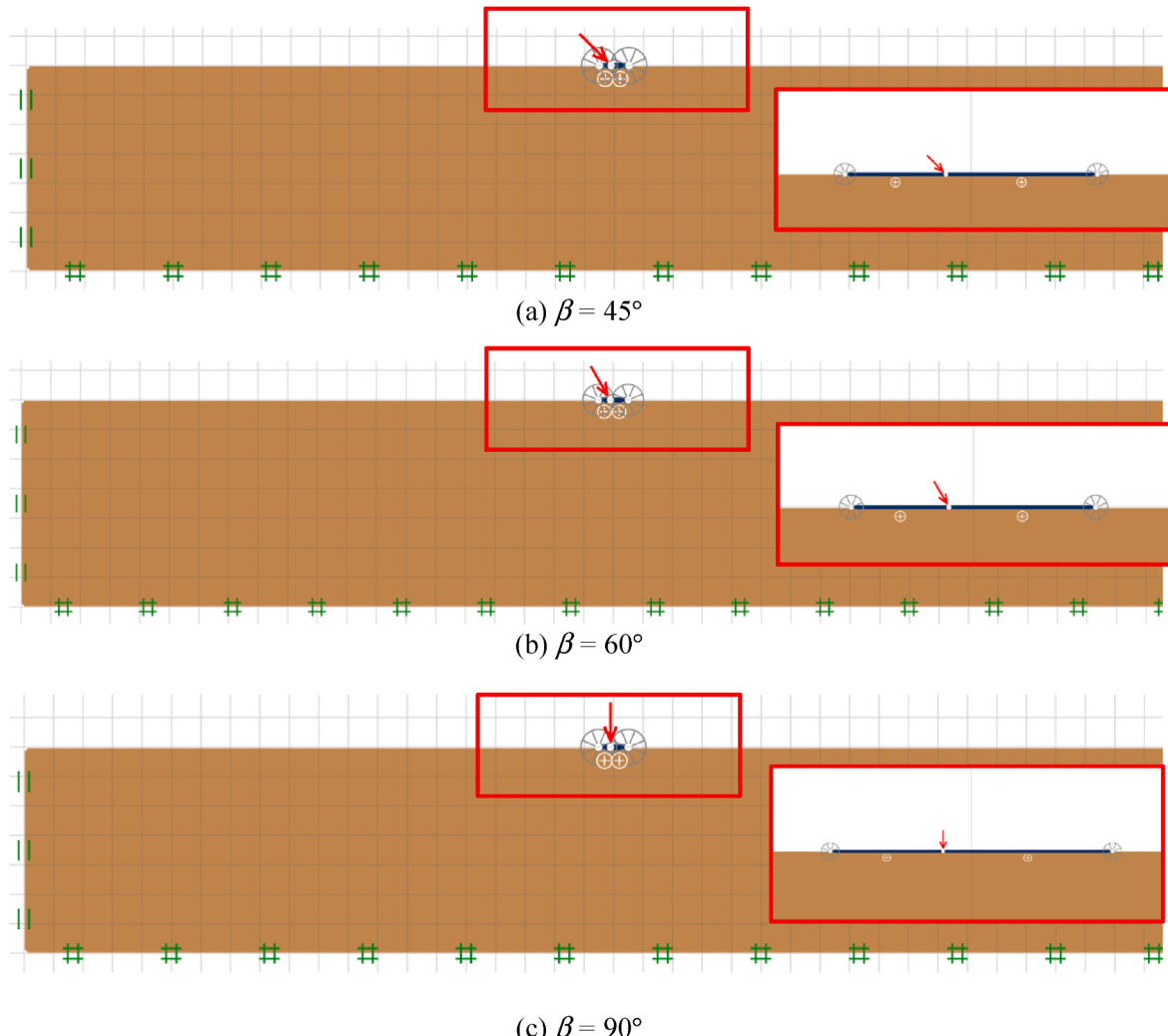


Fig. 2. Typical model geometries for strip footings on AUS clay.
($e/B = 0.1$, $\alpha = 0.25$ and $r_e = 0.5$).

the footing to expand the reliability of the calculation, which enhances the accuracy of the computed numerical results.

Determining the precise ultimate load with eccentricity and inclination operating on the strip footing is the prime objective of lower bound analysis as well as upper bound analysis. Consequently, the FELA software has a powerful function known as adaptive mesh refinement which was developed by Ciria et al. (2008), to minimize inaccuracy while improving the precision of the results. In order to greatly enhance the computational effectiveness of all models, adaptive meshing techniques are employed where the number of elements is consequently automatically raised in the zones having high plastic shear strains. The closer UB and LB solutions are produced as the disparities between UB and LB solutions get reduced after a few iteration stages (Ukrichon and Keawsawasvong, 2017, 2018; Keawsawasvong and Ukrichon, 2017a-c, 2019, Keawsawasvong et al., 2021b, Shiu et al., 2021, Yodsomjai et al., 2021b-c). The adaptive mesh refinement technique employed in this study is a sophisticated feature of OptumCE, as described by Ciria et al. (2008). It utilizes an automated approach for adaptive mesh refinement, expanding the mesh in areas with significant plastic shearing strain. All analyses implement a value proposed in the software recommendations using three adaptive iterations phases, guaranteeing that this value is sufficient to produce a precise response. Over the span of three adaptivity iteration phases, a starting mesh with 3000 elements is gradually enlarged to a finalized mesh of 5000 elements. Increasing the number of elements can enhance sensitivity to stress zones and provide a more precise solution. However, exceeding 5000 elements is unnecessary as it

has little impact on the solution while consuming additional CPU time and computer memory. It is worth noting that employing this adaptive mesh refinement setting ensures that the lower bound (LB) and upper bound (UB) solutions are extremely close, indicating that the true solutions can be obtained. An illustration of typical adaptive meshes of a strip footing on anisotropic undrained clay after three iterations are shown in Fig. 3. It is evident that the number of meshes considerably rises in the region with substantial plastic shear strains, which can reveal the failure mechanisms of the clay layer.

4. Results and discussions

The parametric analyses are conducted to investigate the impact of each parameter on the bearing capacity factor of a strip footing on anisotropic clay under eccentric and inclined loading. The numerical outcomes are expressed using the average (AVG) results derived from UB and LB solutions. Firstly, the influence of β on the bearing capacity factor solutions ($P/s_{uc}B$) with the selected value of $e/B = 0.1$ and 0.4 are demonstrated in Fig. 4(a–b), respectively. The charts contain a sample of other considered dimensionless parameters including various r_e values between 0.5 and 1.0 with the specific value of $\alpha = 1.0$. According to the numerical results, the increase in inclination angle leads to a greater value of the bearing capacity factor in all cases. It clearly indicates that since β getting larger, the horizontal forces are reduced, while $\beta = 90^\circ$ leads to the greatest bearing capacity of the footing due to the horizontal forces being neglected thus only vertical loads are considered. On the

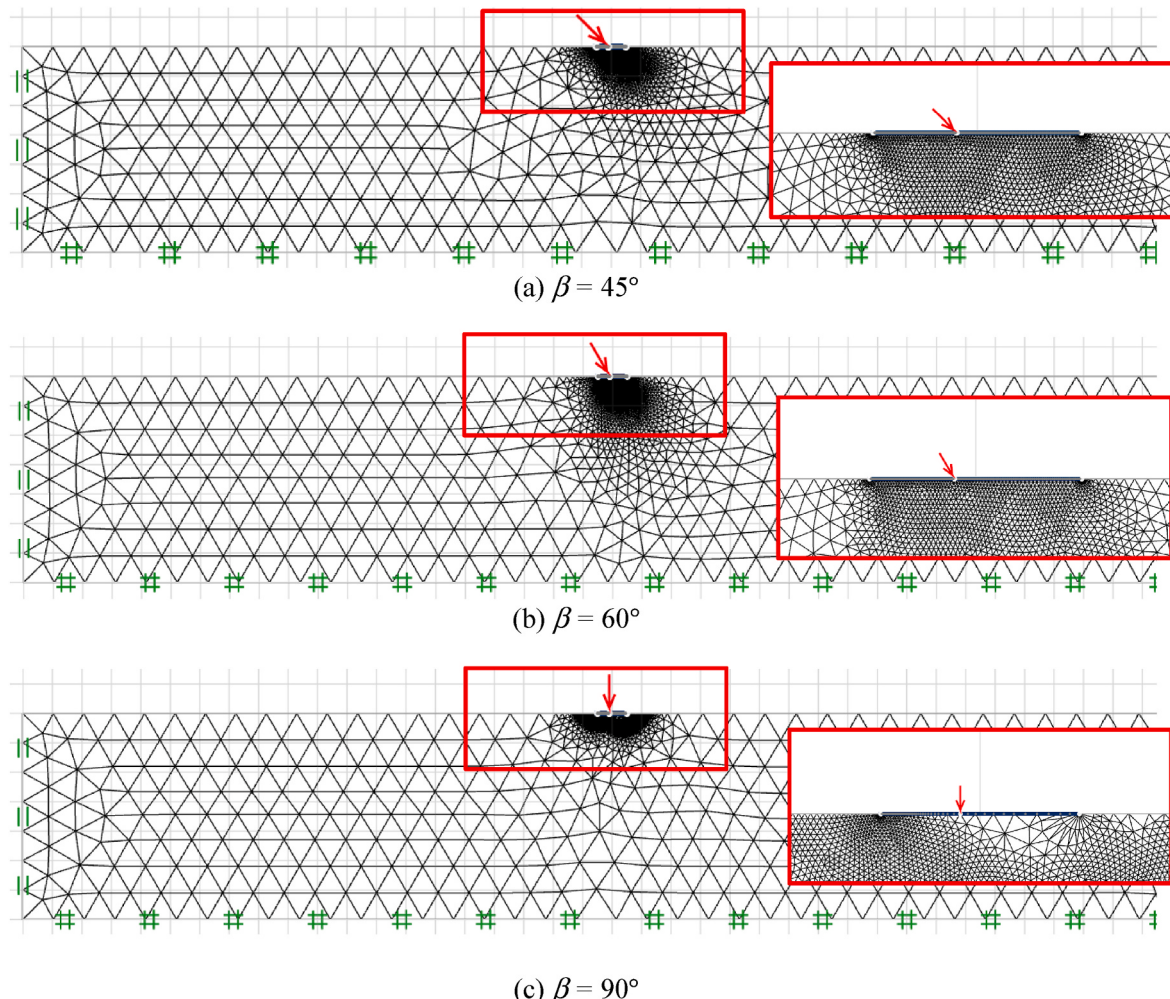


Fig. 3. Typical adaptive meshes for strip footings on AUS clay.
($e/B = 0.1$, $\alpha = 0.25$ and $r_e = 0.5$).

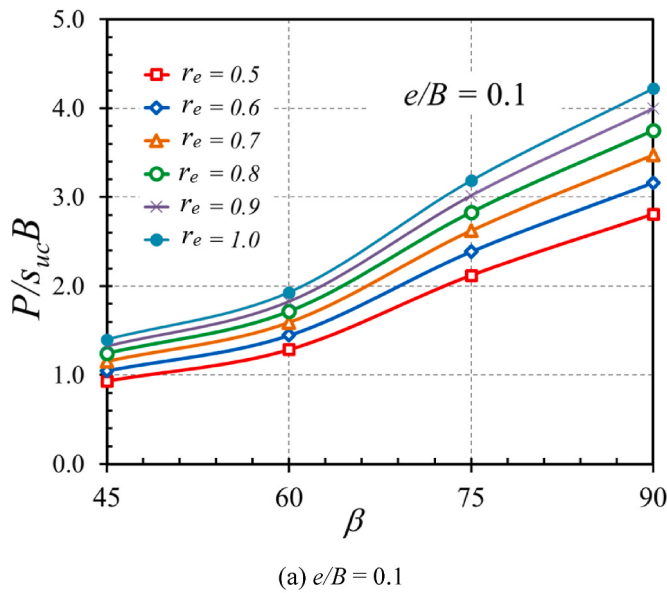
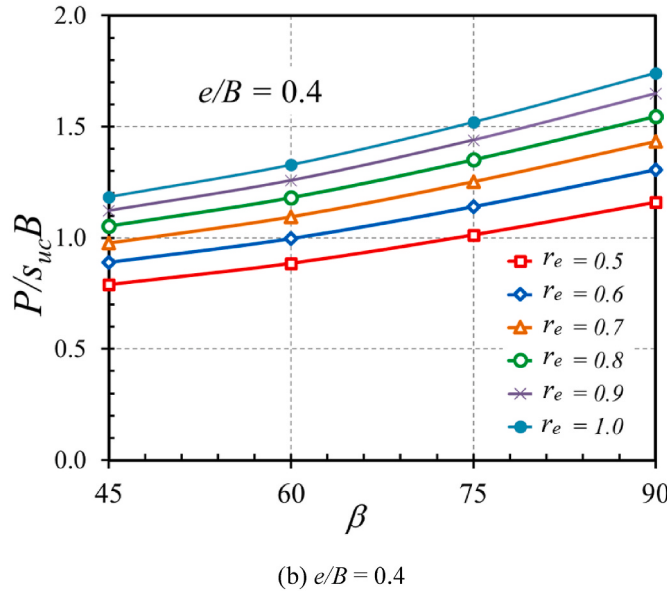
(a) $e/B = 0.1$ (b) $e/B = 0.4$

Fig. 4. Influence of β on the solutions of bearing capacity of footing on the AUS clay ($\alpha = 1$).

other hand, due to the horizontal force produced by the inclined angle, the bearing capacity factor likewise decreases as β approaches zero. Furthermore, the influence of e/B on the bearing capacity factor solutions ($P/s_{uc}B$) with the selected value of $\beta = 45^\circ$ and 90° are demonstrated in Fig. 5(a-b), respectively. A non-linear reducing relationship between e/B and $P/s_{uc}B$ is observed in all cases. This happens due to the fact that a high eccentric length often reduces the effectiveness of the force imparted to the footing. Note that for the small inclination angle $\beta = 45^\circ$, the variation of e/B has not much influence on $P/s_{uc}B$. The influence of α on the bearing capacity factor solutions ($P/s_{uc}B$) is plotted in Fig. 6(a-b). The plots contain four values of $e/B = 0\text{--}0.4$ and other dimensionless parameters are set as $r_e = 0.5$ and 1.0 with $\beta = 90^\circ$. As seen in both Fig. 6(a-b), the variation of α have no significant influence on the bearing capacity factor therefore the strip footing's bearing capacity is unaffected by the contact surface's roughness. Lastly, Fig. 7 (a-b) demonstrated the influence of r_e on the bearing capacity factor solutions ($P/s_{uc}B$). The plots are computed with four values of $\alpha = 0.25\text{--}1.0$ and other dimensionless parameters are set as $e/B = 0.1$ and 0.4 with $\beta = 45^\circ$. A non-linear increasing relationship between r_e and $P/s_{uc}B$ can be founded in all cases while the increasing gradient directly depends on the roughness surface. Besides that, the highest value of $P/s_{uc}B$ is obtained when $r_e = 1$ which indicates the isotropic characteristics of the clay around the footing.

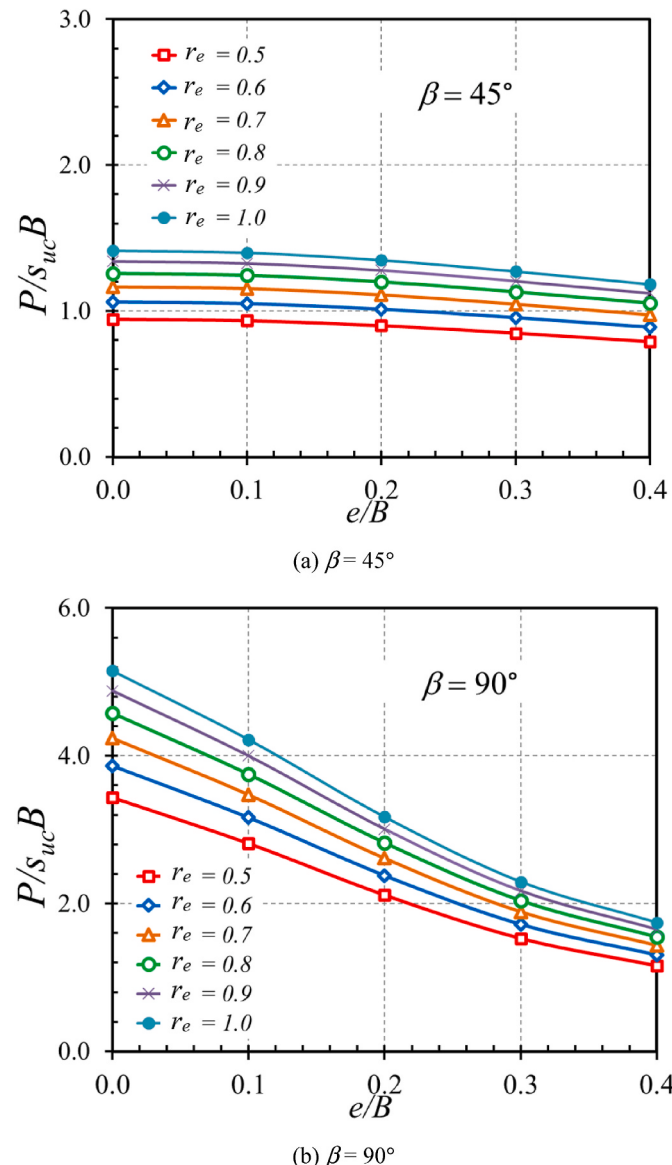
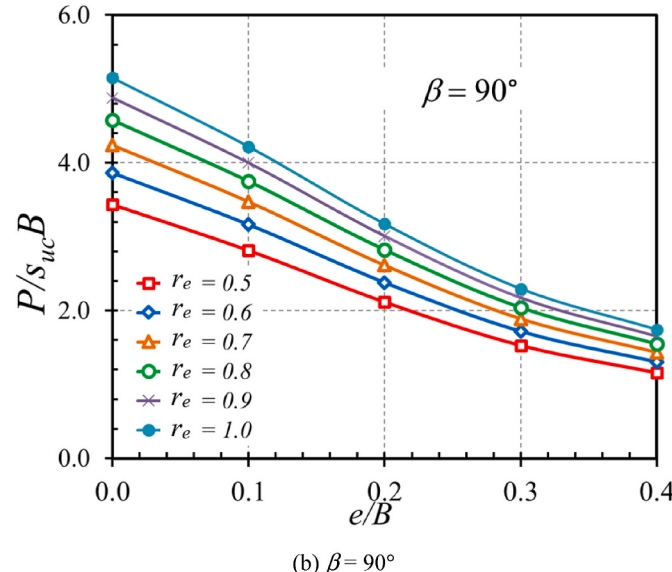
(a) $\beta = 45^\circ$ (b) $\beta = 90^\circ$

Fig. 5. Influence of e/B on the solutions of bearing capacity of footing on the AUS clay ($\alpha = 1$).

$s_{uc}B$ can be founded in all cases while the increasing gradient directly depends on the roughness surface. Besides that, the highest value of $P/s_{uc}B$ is obtained when $r_e = 1$ which indicates the isotropic characteristics of the clay around the footing.

5. New proposed MOGA-EPR model

A new model has been developed in this section to enable easy estimation of the strip footing's bearing capacity factor. The model has been developed using the multi objective evolutionary polynomial regression analysis (MOGA-EPR) method, which is a method based on regression analysis and artificial intelligence (Giustolisi and Savic, 2009). This method has been proven to provide accurate and robust design equations in the field of geotechnical engineering (Alzabeebee, 2022; Alzabeebee et al., 2022a, 2022b). The accuracy of the equations is measured using the coefficient of determination (R^2). The MOGA-EPR method divides the data into training and testing sets, and the R^2 values are calculated for both sets to ensure that the equation can predict the results of data that were not used in its development. Note that other artificial intelligence techniques have been used to predict the bearing

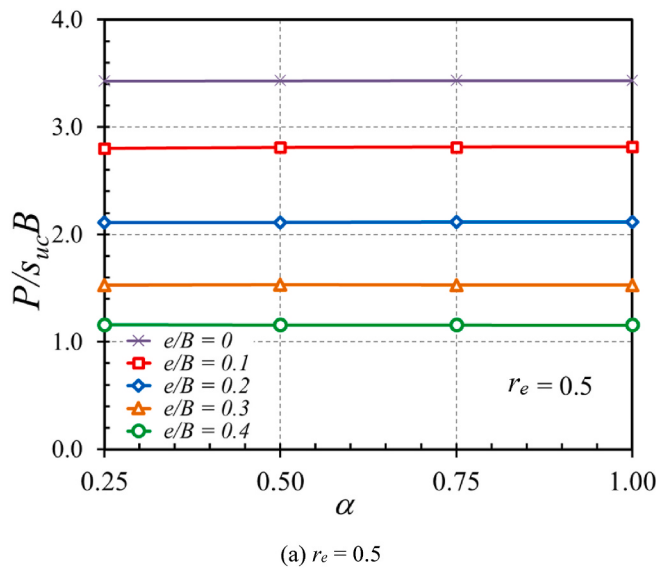
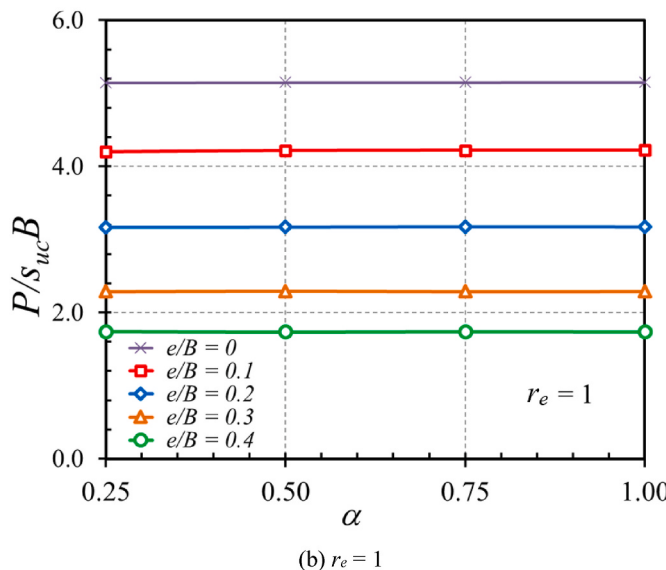
(a) $r_e = 0.5$ (b) $r_e = 1$

Fig. 6. Influence of α on the solutions of bearing capacity of footing on the AUS clay ($\beta = 90^\circ$).

capacity of footings and piles by some previous works such as Ibrahim et al. (2023), Kumar et al. (2022), Lai et al. (2022b; 2022c), and Van et al. (2022).

The data used in the MOGA-EPR analysis were arranged as dependent variable (the strip footing's bearing capacity factor in anisotropic clay under eccentric and inclined loads) and the associated independent variables [r_e (the anisotropic strength ratio), e/B (the dimensionless eccentricity), α (the adhesion factor), and β (the load inclination angle)]. The data were divided into training and testing sets, with 80% of the data used for training and 20% used for testing. The statistical measures of the training and testing data were calculated to ensure that the testing data were within the range of the training data as shown in Tables 2 and 3.

The equation developed using the MOGA-EPR analysis for predicting the strip footing's bearing capacity factor is shown in Eqn 5.

$$\begin{aligned} \text{Bearing capacity factor} = & A\beta^{1.5}\sqrt{r_e} + B\beta^2\sqrt{r_e} + C\sqrt{r_e}\alpha\beta + D\beta^2\sqrt{r_e}\alpha\left(\frac{e}{B}\right) \\ & + E\beta\sqrt{r_e}\alpha\left(\frac{e}{B}\right)^{1.5} + F \end{aligned} \quad (5)$$

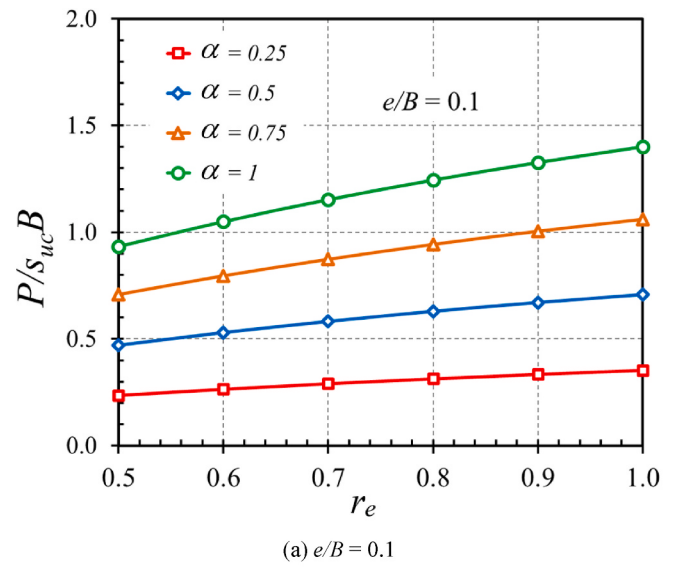
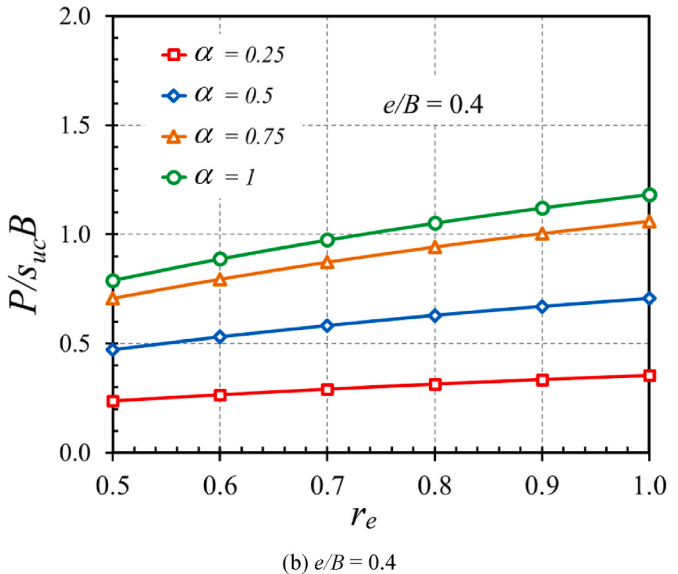
(a) $e/B = 0.1$ (b) $e/B = 0.4$

Fig. 7. Influence of r_e on the solutions of bearing capacity of footing on the AUS clay ($\beta = 45^\circ$).

Table 2
Statistical measures of the training data.

Statistical measure	r_e	e/B	α	β	$P/SucB$
Minimum	0.50	0.00	0.25	45.00	0.24
Maximum	1.00	0.40	1.00	90.00	4.22
Average	0.76	0.2	0.64	68.01	1.46
Standard deviation	0.17	0.11	0.28	16.86	0.89

Table 3
Statistical measures of the testing data.

Statistical measure	r_e	e/B	α	β	$P/SucB$
Minimum	0.50	0.0	0.25	45.00	0.24
Maximum	1.00	0.40	1.00	90.00	4.22
Average	0.72	0.2	0.58	65.45	1.21
Standard deviation	0.18	0.12	0.27	16.49	0.80

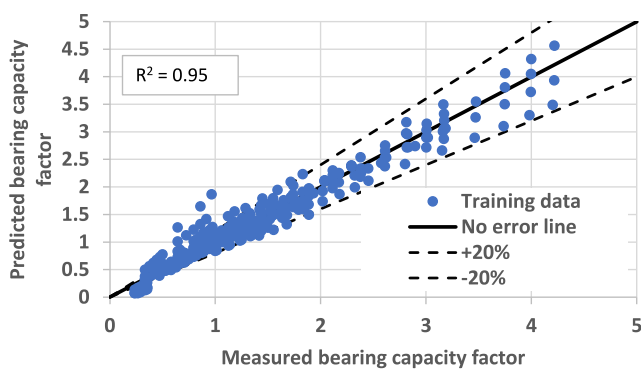


Fig. 8. Comparison between measured and predicted bearing capacity factor for the training data.

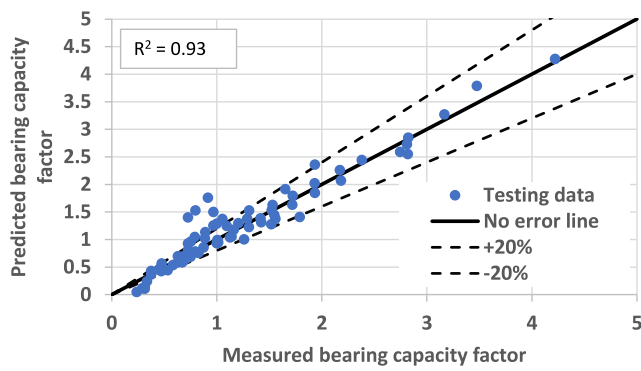


Fig. 9. Comparison between measured and predicted bearing capacity factor for the testing data.

where A, B, C, D, F are the constant coefficients consist of $-0.0169, 0.0021, 0.4019, -0.0027, 0.1816$, and -0.1808 , respectively.

Figs. 8 and 9 compare the relationship between predicted and measured bearing capacity factor with the no error line and error range of $\pm 20\%$. The obtained R^2 values are also presented in Figs. 8 and 9. It is evident from the figures that the new model achieved robust estimation with very high R^2 values for both training (0.95) and testing (0.93). Thus, the developed model could be used with confidence based on the accuracy examinations presented in this paper. Importantly, it should be stated that new model should be used for designs within the range of anisotropic strength ratio, dimensionless eccentricity, adhesion factor and inclination angle listed in Table 3 to ensure accurate results.

6. Conclusion

The bearing capacity solution for the strip footing in anisotropic clay under eccentric and inclined load situations was provided in this paper. The AUS model is used in the numerical computation to describe the characteristics of the clay and the failure criterion based on the FELA approaches. The influences of the four dimensionless parameters which consist of the anisotropic strength ratio, dimensionless eccentricity, the load inclination angle and the adhesion factor are investigated using upper and lower bound FELA methods, leading to the bearing capacity factor ($P/s_{uc}B$). Based on the analytical data and conclusions, the bearing capacity factor increases as the inclination angle and anisotropic strength ratio increase, while it decreases with reducing eccentric length. However, the adhesion factor has a relatively minor effect on the bearing capacity factor. This observation can be explained by considering that as the inclination angle approaches 90° , the horizontal force acting on the footing becomes negligible. Consequently, the impact of

the horizontal force on the footing is disregarded, leading to a reduced influence of the adhesion factor on the bearing capacity. In other words, the adhesion factor has a less significant role when the horizontal force becomes negligible compared to the vertical force. Moreover, the increasing anisotropic strength ratio also resulting in a higher bearing capacity factor due to the isotropic clay properties while the increasing in eccentric length leads to a lower value of bearing capacity factor, this happens due to the facts that a high eccentric length often reduces the effectiveness of the force imparted to the footing. Importantly, a new novel model has been developed in this study to estimate the strip footing's bearing capacity factor in anisotropic clay under eccentric and inclined loads. The new model has been developed using advanced data driven method and is proven to have the capabilities of accurate estimation of the bearing capacity factor for data that has not been used in its development. The solutions presented in this study are specifically applicable to strip footing in anisotropic clay. They cannot be directly extended to analyze multiple footings, raft or mat footing, footings on layered soils, or other footing shapes (i.e. triangular or rectangular footings). However, in future studies, it would be beneficial to include the seismic loading to account for strip footing and investigate the behavior in such configurations. These potential avenues for future research would help expand the applicability of the findings and provide insights into the behavior of footing in different types of geometries and soil conditions.

Data availability statement

All data, models, and code that support the findings of this study are available from the corresponding author upon reasonable request.

Declaration of competing interest

The authors declare that they have no known competing financial interests or personal relationships that could have appeared to influence the work reported in this paper.

Acknowledgement

This study was financially supported by Office of the Permanent Secretary, Ministry of Higher Education, Science, Research and Innovation under Research Grant for New Scholar (RGNS 65–112). The first author would like to thank Faculty of Engineering, Thammasat School of Engineering, Thammasat University, for the graduate scholarship.

References

- Alzabeebee, S., 2022. Explicit soft computing model to predict the undrained bearing capacity of footing resting on aggregate pier reinforced cohesive ground. *Innovative Infrastructure Solutions* 7 (1), 105.
- Alzabeebee, S., Jamei, M., Hasanipanah, M., Amniah, H.B., Karbasi, M., Keawsawasvong, S., 2022a. Development of a new explicit soft computing model to predict the blast-induced ground vibration. *Geomechanics and Engineering* 30 (6), 551–564.
- Alzabeebee, S., Mohammed, D.A., Alshikani, Y.M., 2022b. Experimental study and soft computing modeling of the unconfined compressive strength of limestone rocks considering dry and saturation conditions. *Rock Mech. Rock Eng.* 55 (9), 5535–5554.
- Casagrande, A., Carillo, N., 1944. Shear failure of anisotropic soils. *Contributions to Soil Mechanics (BSCE)* 1941–1953, 122–135.
- Ciria, H., Peraire, J., Bonet, J., 2008. Mesh adaptive computation of upper and lower bounds in limit analysis. *Int. J. Numer. Methods Eng.* 75, 899–944.
- Giustolisi, O., Savic, D.A., 2009. Advances in data-driven analyses and modelling using EPR-MOGA. *J. Hydroinf.* 11 (3–4), 225–236.
- Hansen, J.B., 1970. A Revised and Extended Formula for Bearing Capacity, 28. Bull Danish Geotechnical Institute, pp. 5–11. <https://doi.org/10.3208/sandf1972.33.169>.
- Hjiaj, M., Lyamin, A.V., Sloan, S.W., 2004. Bearing capacity of a cohesive-frictional soil under non-eccentric inclined loading. *Comput. Geotech.* 31 (6), 491–516. <https://doi.org/10.1016/j.compgeo.2004.06.001>
- Ibrahim, A.S., Musa, A.A., Abdulfatah, A.Y., et al., 2023. Developing soft-computing regression model for predicting soil bearing capacity using soil index properties. *Model. Earth Syst. Environ.* 9, 1223–1232.

- Jearシリปองกุล, T., Lai, V.Q., Keawsawasvong, S., Nguyen, T.S., Van, C.N., Thongchom, C., Nuaklong, P., 2022. Prediction of uplift capacity of cylindrical caissons in anisotropic and inhomogeneous clays using multivariate adaptive regression splines. *Sustainability* 14 (8), 4456.
- Keawsawasvong, S., 2022. Bearing capacity of conical footings on clays considering combined effects of anisotropy and non-homogeneity. *Ships Offshore Struct.* 17 (1), 2317–232.
- Keawsawasvong, S., Shiau, J., Ngamkhanong, C., Qui Lai, V., Thongchom, C., 2022. Undrained stability of ring foundations: axisymmetry, anisotropy, and nonhomogeneity. *Int. J. GeoMech.* 22 (1) [https://doi.org/10.1061/\(ASCE\)GM.1943-5622.0002229](https://doi.org/10.1061/(ASCE)GM.1943-5622.0002229).
- Keawsawasvong, S., Thongchom, C., Likitlersuang, S., 2021b. Bearing capacity of strip footing on Hoek-Brown rock mass subjected to eccentric and inclined loading. *Transportation Infrastructure Geotechnology* 8, 189–200.
- Keawsawasvong, S., Ukrritchon, B., 2017a. Undrained limiting pressure behind soil gaps in contiguous pile walls. *Comput. Geotech.* 83, 152–158.
- Keawsawasvong, S., Ukrritchon, B., 2017b. Finite element analysis of undrained stability of cantilever flood walls. *Int. J. Geotech. Eng.* 11 (4), 355–367.
- Keawsawasvong, S., Ukrritchon, B., 2017c. Undrained lateral capacity of I-shaped concrete piles. *Songklanakarin J. Sci. Technol.* 39 (6), 751–758.
- Keawsawasvong, S., Ukrritchon, B., 2019. Undrained stability of a spherical cavity in cohesive soils using finite element limit analysis. *J. Rock Mech. Geotech. Eng.* 11 (6), 1274–1285.
- Keawsawasvong, S., Ukrritchon, B., 2022. Design equation for stability of a circular tunnel in an anisotropic and heterogeneous clay. *Undergr. Space* 7 (1), 76–93.
- Keawsawasvong, S., Yoonirundorn, K., Senjuntichai, T., 2021a. Pullout capacity factor for cylindrical suction caissons in anisotropic clays based on Anisotropic Undrained Shear failure criterion. *Transportation Infrastructure Geotechnology* 8 (4), 629–644.
- Krabbenhoft, K., Galindo-Torres, S.A., Zhang, X., Krabbenhoft, J., 2019. AUS: anisotropic undrained shear strength model for clays. *Int. J. Numer. Anal. Methods GeoMech.* 43 (17), 2652–2666.
- Krabbenhoft, S., Damkilde, L., Krabbenhoft, K., 2014. Bearing capacity of strip footings in cohesionless soil subject to eccentric and inclined loads. *Int. J. GeoMech.* 14 (3), 04014003 [https://doi.org/10.1061/\(ASCE\)GM.1943-5622.0000332](https://doi.org/10.1061/(ASCE)GM.1943-5622.0000332).
- Krabbenhoft, S., Damkilde, L., Krabbenhoft, K., 2012. Lower bound calculations of the bearing capacity of eccentrically loaded footings in cohesionless soil. *Can. Geotech. J.* 49 (3), 298–310. <https://doi.org/10.1139/t11-103>, 2012.
- Kumar, M., Kumar, V., Rajagopal, B.G., et al., 2022. State of art soft computing based simulation models for bearing capacity of pile foundation: a comparative study of hybrid ANNs and conventional models. *Model. Earth Syst. Environ.*
- Ladd, C.C., DeGroot, D.J., 2003. Recommended practice for soft ground site characterization, Arthur Casagrande Lecture. In: Proceedings of the 12th Panamerican Conference on Soil Mechanics and Geotechnical Engineering, Cambridge.
- Ladd, C.C., 1991. Stability evaluations during stage construction. *Journal of Geotechnical Engineering* 117 (4), 540–615.
- Lai, V.Q., Banyong, R., Keawsawasvong, S., 2022a. Undrained sinkhole collapse in anisotropic clays. *Arabian J. Geosci.* 15 (8).
- Lai, V.Q., Banyong, R., Keawsawasvong, S., 2022e. Stability of limiting pressure behind soil gaps in contiguous pile walls in anisotropic clays. *Eng. Fail. Anal.* 222 (134), 106049.
- Lai, V.Q., Chenari, R.J., Banyong, R., Keawsawasvong, S., 2023. Undrained stability of opening in underground walls in anisotropic clays. *Int. J. GeoMech.* 23 (2).
- Lai, V.Q., Nguyen, D.K., Banyong, R., Keawsawasvong, S., 2021. Limit analysis solutions for stability factor of unsupported conical slopes in clays with heterogeneity and anisotropy. *International Journal of Computational Materials Science and Engineering* 11 (1).
- Lai, V.Q., Kounlavong, K., Keawsawasvong, S., Banyong, R., Wipulanusat, W., Jamsawang, P., 2023a. Undrained basal stability of braced circular excavations in anisotropic and non-homogeneous clays. *Transportation Geotechnics*.
- Lai, V.Q., Shiau, J., Keawsawasvong, S., Seehavong, S., Cabangon, L.T., 2022d. Undrained stability of unsupported rectangular excavations: anisotropy and non-homogeneity in 3D. *Buildings* 12 (9), 142.
- Lai, V.Q., Shiau, J., Keawsawasvong, S., Tran, D.T., 2022b. Bearing capacity of ring foundations on anisotropic and heterogenous clays ~ FEA, NGI-ADP, and MARS. *Geotech. Geol. Eng.* 40, 3929–3941.
- Lai, V.Q., Shiau, J., Van, C.N., Tran, H.D., Keawsawasvong, S., 2022c. Bearing capacity of conical footing on anisotropic and heterogeneous clays using FEA and ANN. *Mar. Georesour. Geotechnol.*
- Lo, K.Y., 1965. Stability of slopes in anisotropic soils. *J. Soil Mech. Found. Div.* 31, 85–106.
- Loukidis, D., Chakraborty, T., Salgado, R., 2008. Bearing capacity of strip footings on purely frictional soil under eccentric and inclined loads. *Can. Geotech. J.* 45 (6), 768–787. <https://doi.org/10.1139/T08-015>.
- Meyerhof, G.G., 1963. Some recent research on the bearing capacity of foundations. *Can. Geotech. J.* 1 (1), 16–26. <https://doi.org/10.1139/t63-003>.
- Meyerhof, G.G., 1955. The bearing capacity of foundations under eccentric and inclined loads. In: Proceedings of the Third Conference of Soil Mechanics, pp. 440–445. <https://doi.org/10.1179/1939787915Y.0000000003>.
- Nguyen, D.K., Nguyen, T.P., Keawsawasvong, S., Lai, V.Q., 2022. Vertical uplift capacity of circular anchors in clay by considering anisotropy and non-homogeneity. *Transportation Infrastructure Geotechnology* 9, 653–672.
- Nguyen, D.K., Nguyen, T.P., Ngamkhanong, C., Keawsawasvong, S., Lai, V.Q., 2023. Bearing Capacity of Ring Footings in Anisotropic Clays: FELA and ANN. *Neural Computing and Applications*.
- Shiau, J., Chudal, B., Mahalingasivam, K., Keawsawasvong, S., 2021. Pipeline burst-related ground stability in blowout condition. *Transportation Geotechnics* 29, 100587.
- Shiau, J., Lai, V.Q., Keawsawasvong, S., 2022. Multivariate adaptive regression splines analysis for three-dimensional slope stability in anisotropic and heterogenous clay. *J. Rock Mech. Geotech. Eng.*
- Sloan, S.W., 2013. Geotechnical stability analysis. *Geotechnique* 63 (7), 531–572. <https://doi.org/10.1680/geot.12.RL.001>.
- Taiebat, H.A., Carter, J.P., 2002. Bearing capacity of strip and circular foundations on undrained clay subjected to eccentric loads. *Geotechnique* 52 (1), 61–64. <https://doi.org/10.1680/geot.52.1.61.40828>.
- Terzaghi, K., 1943. *Theoretical Soil Mechanics*. Wiley, New York.
- Ukrritchon, B., Keawsawasvong, S., 2017. Unsafe error in conventional shape factor for shallow circular foundations in normally consolidated clays. *Journal of Geotechnical and Geoenvironmental Engineering, ASCE* 143 (6), 02817001.
- Ukrritchon, B., Keawsawasvong, S., 2018. Undrained lateral capacity of rectangular piles under a general loading direction and full flow mechanism. *KSCE J. Civ. Eng.* 22 (7), 2256–2265.
- Van, C.N., Keawsawasvong, S., Nguyen, D.K., Lai, V.Q., 2022. Machine learning regression approach for analysis of bearing capacity of conical footings in heterogenous and anisotropic clay. *Neural Comput. Appl.*
- Vesic, A., 1975. Bearing capacity of shallow foundations. In: Winterkorn, H.F., Fang, H.Y. (Eds.), *Foundation Engineering Handbook*. Van Nostrand Reinhold, New York, pp. 121–147. https://doi.org/10.1007/978-1-4757-5271-7_14.
- Yodsomjai, W., Keawsawasvong, S., Senjuntichai, T., 2021a. Undrained stability of unsupported conical slopes in anisotropic clays based on AUS failure criterion. *Transportation Infrastructure Geotechnology* 8 (4), 557–568.
- Yodsomjai, W., Keawsawasvong, S., Senjuntichai, T., 2021b. Undrained stability of unsupported conical slopes in anisotropic clays based on Anisotropic Undrained Shear failure criterion. *Transportation Infrastructure Geotechnology* 8 (4), 557–568.
- Yodsomjai, W., Keawsawasvong, S., Thongchom, C., Lawongkerd, J., 2021c. Undrained stability of unsupported conical slopes in two-layered clays. *Innovative Infrastructure Solutions* 6, 15.
- Zheng, G., Zhao, J., Zhou, H., Zhang, T., 2019. Ultimate bearing capacity of strip footings on sand overlying clay under inclined loading. *Comput. Geotech.* 106, 266–273.